Kinetics of CO_2 methanation over a Ni/alumina industrial catalyst

By Rogéria Amaral and Sébastien Thomas
Laboratoire de Matériaux, Surfaces et Procédés pour la Catalyse, Groupe Energie et Carburants pour un Environnement Durable, UMR CNRS 7515, Université de Strasbourg, Strasbourg, France

Abstract

The increase of the consumption of renewable energies creates challenges concerning the storage of the excess of electricity produced. One solution is convert hydrogen produced via electrolysis of water and carbon dioxide into methane. This worked focused in the kinetic study and modelling of this reaction named CO_2 methanation. Several catalytic tests were realized to evaluate the influence of the products and reactants involved. After, three kinetic models were proposed for CO_2 methanation and two other reactions that occur in parallel. The kinetic constant were determined and the models tested in a plug flow reactor model.

1 Introduction

With the increasing of the use of renewable sources, the storage of electric energy is a big concern, to provide electricity without the use of batteries, because renewable sources cannot provide base load electric power due to their intermittent nature (e.g., wind energy). So the excess of electric energy can be converted into chemical energy by transferring it into fuels such as hydrogen, synthetic natural gas (SNG) or methanol through the “Power to Gas” system. By converting CO_2 into methane (CO_2 methanation) using hydrogen produced via electrolysis of water (ideally with the excess of electric energy from renewable sources) it is avoided the liberation of this gas to atmosphere and provides methane for electricity production.

The reaction involved in this process is described by:

$$CO_{2(g)} + 4H_{2(g)} \rightarrow CH_{4(g)} + 2H_2O_{(g)} \quad (1)$$

This is the Sabatier reaction observed by Paul Sabatier over a Nickel catalyst in 1902. It has a heat reaction, $\Delta_r H_{298K}^o$, of -165 kJ.mol^{-1} and it is typically operated at temperatures between 200ºC and 550ºC depending on the catalyst used. [1]

Recently, much research has been made in order to find a catalyst for CO_2 methanation. These studies have provided significant information about the reaction kinetics and thermodynamic behaviours. However, little is yet known about the reaction mechanism of carbon dioxide methanation.

Accordingly with the study of Bartholomew *et al* [2], the kinetic model of the methanation of CO_2 is based on a complex Langmuir-Hinshelwood mechanism involving dissociative adsorption of CO_2 to CO and atomic oxygen followed by hydrogenation of CO via a carbon intermediate to methane. It was considered the CO dissociation as the rate-determining step and the adsorption of CO_2 and H_2 and the desorption of CO as the formation of a hydroxide are in quasi-equilibrium.

The equation reached was the only rate expression that resulted in physically meaningful rate and adsorption equilibrium constants as well as a linear Arrhenius plot for the rate constant k_4.

$$r_{CH_4} = \frac{\left(\frac{K_1 K_2 K_{10} k_4 k_{11}}{2}\right)^{1/2} L^2 P_{CO_2}^{1/2} P_{H_2}^{1/2}}{\left(1 + \left(\frac{2K_2 k_4}{K_1 K_{10} k_{11}}\right)^{1/2} \frac{P_{CO_2}^{1/2}}{P_{H_2}^{1/2}} + \left(\frac{K_1 K_2 K_{10} k_{11}}{2k_4}\right)^{1/2} P_{CO_2}^{1/2} P_{H_2}^{1/2} + \frac{P_{CO}}{K_3}\right)^2} \tag{2}$$

The conclusions of the study are that the rate of CO_2 hydrogenation on Ni/SiO_2 is quite sensitive to reactant concentrations at low H_2 and CO_2 partial pressures while reaction orders approach zero for H_2 and CO_2 at high reactant concentrations.

Also, addition of CO to the reactants above the equilibrium level causes a significant decrease in the rate of CO_2 hydrogenation apparently as a result of product inhibition, since they both adsorb in the same active sites.

Another study analyzed was performed by Froment *et al* [3], at 10 bar and H_2 / CO_2 = 1. From several reactions which may occur only three were proved by experimental results as CO and CO2 methanation and reverse water-gas shift.

The rate equation for CO_2 methanation was written for the rate-determining step in terms of the concentration of the adsorbed species.

$$r_{17} = \frac{k_3}{P_{H_2}^{3,5}} \left(P_{CH_4} p_{H_2O}^2 - \frac{P_{H_2}^4 P_{CO_2}}{K_3} \right) / (DEN)^2 \tag{3}$$

$$\text{DEN} = 1 + K_{CO} P_{CO} + K_{H_2} P_{H_2} + K_{CH_4} P_{CH_4} + K_{H_2O} P_{H_2O} / P_{H_2} \tag{4}$$

In the article of Wheeler *et al* [4], the mechanism of water-gas shift on a noble metal is assumed to consist of elementary steps such as adsorption and desorption of CO, H_2O, CO_2 and H_2 and surface reactions.

With Langmuir isotherms for all species, the rate becomes

$$r'' = \frac{k_f'' K_{CO} K_{H_2O} P_{CO} P_{H_2O} - k_b'' K_{CO_2} K_{H_2} P_{CO_2} P_{H_2}}{(1 + K_{CO} P_{CO} + K_{H_2O} P_{H_2O} + K_{CO_2} P_{CO_2} + K_{H_2} P_{H_2})^2} \tag{5}$$

2 Experimental

2.1 Catalyst characterization

In this work it was used an industrial powder catalyst named “Octolyst”, provided by CEA sited in Grenoble. It was known the catalyst was composed by Ni aluminate which had undergone a pretreatment under H2 at low temperature which extracts a fraction of Ni out of the structure leading to a system NiO / $NiAl_2O4$ / Al_2O3. Temperature-programmed reduction (TPR) was made to study the reducibility of the catalyst. TPR measurements were carried out with 100 mg of catalyst, loaded in a quartz U-tube and heated under 10% H_2/Ar in three different scenarios: from room temperature to 900ºC at a heating rate of 15ºC.min^{-1}; first step of reduction at 400ºC at a heating rate of 5ºC.min^{-1} during one hour, after coold down under a flow of H_2, to perform the second step of reduction until 900ºC at 15ºC.min^{-1}; and first step of reduction until 500ºC at 5ºC.min^{-1} during one hour, after cool down under a flow of hydrogen to be heated again at 900ºC at a heating rate of 15ºC.min^{-1}. TPR profiles are presented as a function of time herein. The Ni metal surface area (m^2.gcat^{-1}) was calculated from the amount of chemisorbed hydrogen, measured by H_2 temperature programmed desorption (H2-TPD). Prior to H2-TPD, the catalyst (100 mg) was pre-reduced at 400 ºC and 500ºC during one hour at a heating rate of 5ºC.min^{-1} under a 10% H_2/Ar flow and cooled down to 60ºC under pure Ar flow to purge all the hydrogen. Then H_2 chemisorption pulses were performed. The sample was then purged with pure Ar to remove the reversibly adsorbed H_2. The TPD analysis was carried to 900ºC at a heating rate of 15ºC.min^{-1} under pure Ar flow. The specific surface area of the catalyst was determined by N_2 adsorption–desorption measurements at 77 K using the Brunauer–Emmet–Teller (BET) method. X-ray diffraction patterns (XRD) were recorded on a Bruker D8 Advance diffractometer with a LynxEye detector and Ni filtered Cu Kα radiation (1.5418A˚) over a 2θ range of 15–75º and a position sensitive detector using a step size of 0.012º and a step time of 0.05 sec.

2.2 Catalytic activity

The catalysts were reduced in situ before reaction in a 10% H_2/N_2 stream for 1 h with a total gas flow of 50 mL.min^{-1} at 500ºC with a heating ramp of 5ºC.min^{-1}. Carbon dioxide methanation was conducted at atmospheric pressure in a fixed-bed down-flow reactor at a range of temperatures between 325 – 400ºC. The catalyst is placed in a fixed bed between two pieces of quartz wool and diluted in SiC. A thermocouple was placed in contact with the resistance and other thermocouple was placed at the exit of the catalytic bed and it is defined as reaction temperature. The reactor was heated in a tubular furnace monitored by a temperature controller. The flow of components was regulated by calibrated mass flow controllers (Brooks) and N_2 was added as an internal standard. The space velocity was set to 1.9x10^6 h^{-1} with 2 mg of catalyst loaded into the reactor. The feed and products were analyzed on-line by a micro gas chromatograph (Agilent M200H, poraplot U and molecular sieve 5Å columns) equipped with a TCD.

3 Results and discussion

The hydrogen consumption profile of two samples reduced at two different scenarios is shown in Fig.2. It is observed in profile a) that the main reduction occurs at 340ºC correspondent to the nickel present in NiO. The consumption of hydrogen continues up to temperatures as high as 560ºC, accounting for the reduction of the nickel present in the structure nickel alumina.

The profile b), representing the consumption of hydrogen after the pre-reduction at 400ºC, indicates all nickel present in NiO was reduced in the first stage of the analysis. The lack of the peak at 340ºC shows there was no more nickel oxide to reduce, being present only the structure nickel alumina that was reduced at the same temperature observed in the sample a).

Another sample was also reduced in two stages; however the first reduction was performed until 500ºC. It was observed again the typical peak for NiO and a reduction of 47% of the nickel present in nickel alumina translated by the early formation of the peak at 400ºC. As the increasing of the temperature was stopped, the consumption of hydrogen is immediately reduced until approximately zero. As it is not expected temperatures reaction above 500ºC and the reduction at this temperature showed to be stable, this last method was chosen to be performed before any catalytic test.

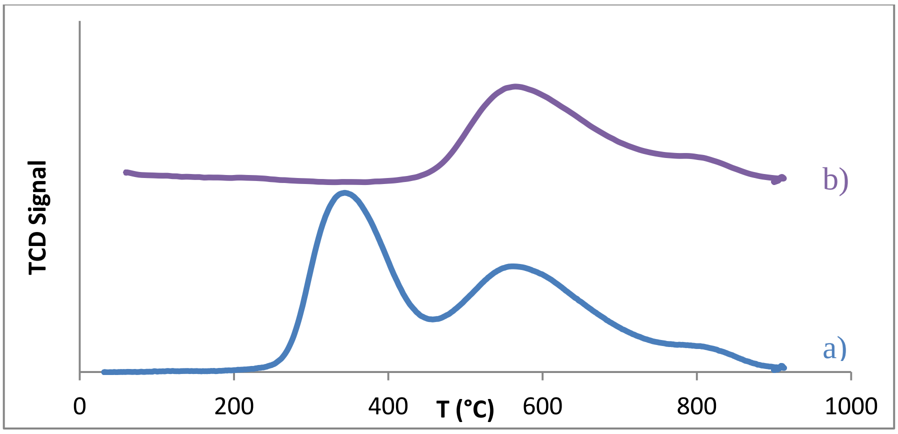

Figure 1: TPR profiles: a) continuous reduction until 900ºC; b) reduction until 900ºC after pre-reduction at 400ºC

The metallic dispersion of nickel and, consequently, particle size of metallic nickel generated by a reducing pre-treatment at 400 and 500ºC have been evaluated by H_2 chemisorption, with the results given in Table 1. When compared the results obtained in XRD, it shows a discrepancy between the two values, which indicates the method applied in XRD was not the most correct or the results obtained in H_2 chemisorption are not reliable.

The diffractograms of the four samples analyzed are shown in Fig.1. It is observed peaks of aluminium oxide at 67º in all the samples in addition to a wide peak at 46º. In that peak includes contribution from metallic nickel and nickel alumina. On the other hand, the peak represented at 37º complies a big contribution of nickel oxide and aluminium oxide. In order to estimate the particle size of nickel, the peak comprised between 40 and 50º was separated in two symmetric peak of nickel and aluminium oxide. Through the peak of nickel, it was possible to apply the equation Scherrer, given the result showed in Table 1.

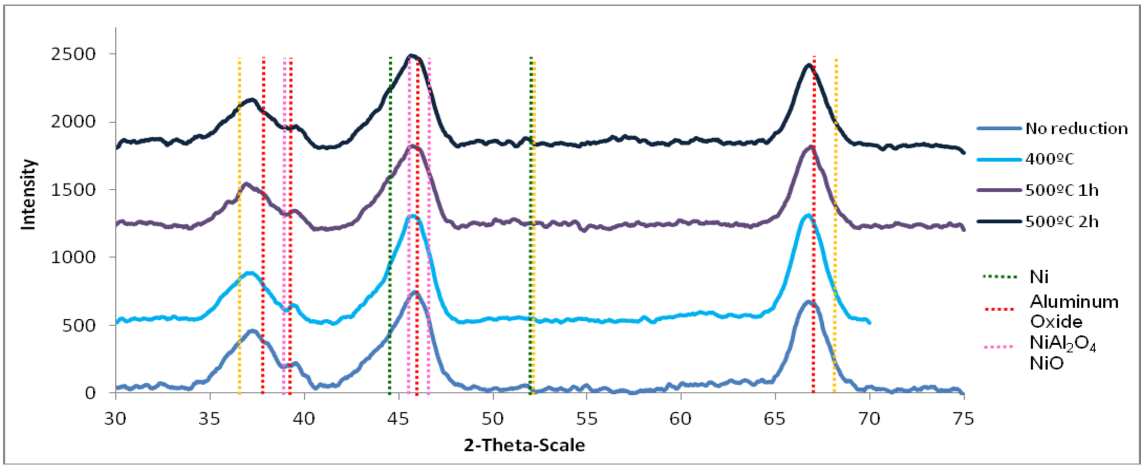

Figure 2: XRD patterns of the four samples analyzed

Finally, the results obtained in N_2 adsorption-desorption measurements show the same structural properties for the sample with different particle size but a difference after the sample be reduced as it can be seen in Table 1, due to the extraction of the nickel from the structure of nickel alumina.

Table 1: Textural characterization of the catalyst

Reduction treatment	400ºC	500ºC	900ºC
Ni reducible$^{a)}$	7.8%	11.0%	14.0%
Dispersion$^{b)}$	8%	5%	
Particle size, d (nm)	10.6$^{b)}$	16.7$^{b)}$ 6.1$^{c)}$	

a) – From TPR-H_2
b) – From H_2 chemisorption
c) – From XRD

Sample	500-315 μm	50-25 μm	200-125 μm after reduction at 500ºC
Surface area (m^2/g)*	246	231	370
Pore diameter (nm)*	8.0	8.0	9.0
Pore volume (cm^3/g)*	0.50	0.50	0.90

* - From N_2 physisorption

After investing the existence of limitations to external and internal diffusion and concluding the formation rate of methane is not influenced neither by the mass of catalyst nor by its particle size, the catalytic tests were performed in order to evaluate the influence of the reactants and products in the kinetics.

The influence of the reactants was analyzed by changing the inlet flow of one of the components while the others were kept constant. It was necessary to add Argon to maintain the total flow. The conversion was kept lower than 20% to assure no influences of the thermodynamic equilibrium and to guarantee no formation of heavier hydrocarbons.

It was performed tests with only CO_2 and also with only CO at the inlet. In the first case, occurs CO_2 methanation and reverse water-gas shift where there is formation of CO and, consequently, occurs CO methanation. However, as the conversion was kept low, this formation is limited. By plotting the formation rate of methane in function of the partial pressure of the reactant that suffered changes it is possible to observe its influence in the reactions of methanation. On the other hand, if it is plotted the formation rate of CO, it concerns the behaviour of the reaction of reverse water-gas shift.

Two examples are represented in the figures 3 and 4, and they show a strong influence of CO_2 in the two reactions referred. In the other experiments, it was also verified a strong influence of CO in CO methanation. In all the reactions, with the exception of RWGS, the hydrogen showed to increase significantly the formation rate of methane when its partial pressure is increased. The observation made for RWGS suggests there is no adsorption of the hydrogen in the active site, or occurs a redox mechanism where the oxidation of hydrogen is must faster than the reduction of CO_2.

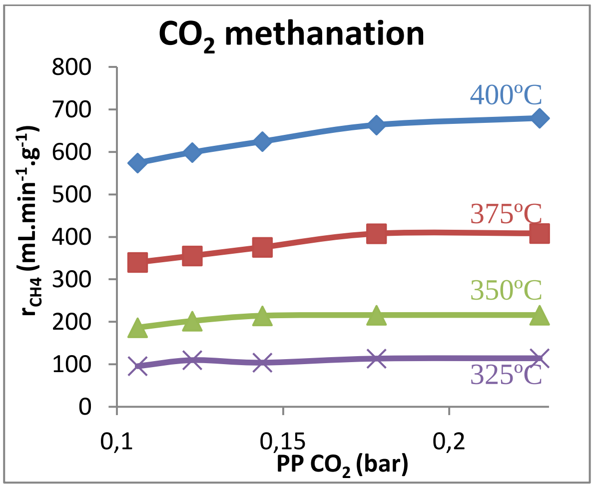

Figure 3: Influence of CO_2 on formation rate of methane in CO_2 methanation

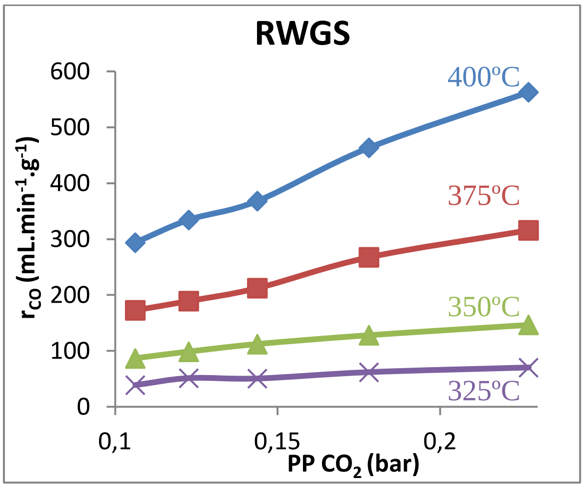

Figure 4: Influence of CO_2 on formation rate of CO in RWGS

The results obtained for CO_2 methanation were tested in the models found in the literature. In the models of Bartholomew *et al* and Xu and Froment there was not a good fitting of the data and/or it showed negative parameters what is impossible as all the models are composed by kinetics constants. The model of Wheeler *et al*, proposed in literature for water-gas shift, showed to have a good fit for the experimental results of CO and CO_2 methanation. The kinetic constants and the adsorption constant of CO, CO_2 and H_2 were calculated. For reverse water-gas shift, it was proposed a redox model and it showed to be appropriate to describe the behaviour of the reaction.

Next it was necessary to test the model in the presence of the products at the inlet. For that it was introduced, separately, water and methane in quantities higher than the one formed by the reactions.

It was observed no influence of methane in all the reactions what it is in accord with the model of Wheeler *et al* and the redox model. However, in the case of water, the model showed a better fit to the data if taken into account its dissociative adsorption. This observation was verified in the model of RWGS.

Finally, it is possible to propose a model for the three reactions in study and to calculate the constants of the equations:

$$r_{CH_4} = \frac{k_{CO_2met}K_{CO_2}K_{H_2}P_{CO_2}P_{H_2}}{\left(1 + K_{CO_2}P_{CO_2} + K_{CO}P_{CO} + K_{H_2}P_{H_2} + K_{H_2O}^{1/2}P_{H_2O}^{1/2}\right)^2} \tag{6}$$

$$r_{CH_4} = \frac{k_{COmet}K_{CO}K_{H_2}P_{CO}P_{H_2}}{\left(1 + K_{CO_2}P_{CO_2} + K_{CO}P_{CO} + K_{H_2}P_{H_2} + K_{H_2O}^{1/2}P_{H_2O}^{1/2}\right)^2} \tag{7}$$

$$r_{CO} = \frac{k_{RWGS}P_{CO_2}}{\left(1 + K_{CO_2}P_{CO_2} + K_{CO}P_{CO} + K_{H_2}P_{H_2} + K_{H_2O}^{1/2}P_{H_2O}^{1/2}\right)} \tag{8}$$

As referred before the kinetic study was performed at low conversion, however it is necessary to evaluate the prediction of the models at higher conversion. For that, new catalytic tests were performed with different masses of catalyst and different flow rates (but with same composition) to simulate a plug flow.

By simulating a plug flow reactor with the models in an excel file, it is possible to plot the experimental data and the data predicted by the models and compared them. Initially, the fitting was not good and so it was performed an adjustment of the constants calculated before (presented in Table 2) in order to have a good fit of the models with the experimental results.

Some examples are showed in the Figs. 5, 6 and 7.

Table 2: Final values of the kinetic constants

	CO_2	**CO**	**H_2**	**H_2O**	**CO_2 methanation**	**CO methanation**	**RWGS**
Qads (kJ/mol)	56.8	121.4	105.1	94.4	-	-	-
K_0 (bar^{-1})	4.7×10^{-6}	2.9×10^{-9}	4.3×10^{-10}	7.6×10^{-7} ($bar^{-1/2}$)	-	-	-
Ea (kJ/mol)	-	-	-	-	242.4	144.0	94.3
k_0 (mol/min.g)	-	-	-	-	1.1×10^{21}	1.9×10^{12}	1.6×10^{7}

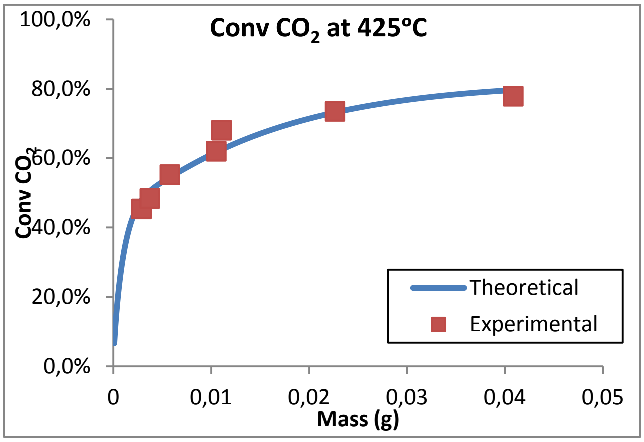

Figure 5: Comparison between the prevision of the conversion of CO_2 at 425ºC by the kinetic model and the experimental results with only CO_2 at the inlet

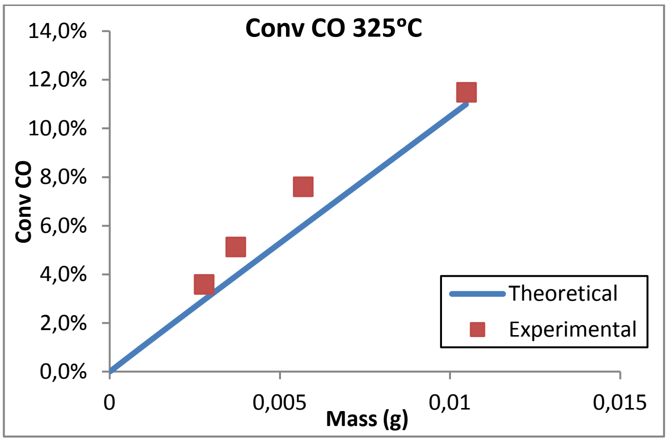

Figure 6: Comparison between the prevision of the conversion of CO at 325ºC by the kinetic model and the experimental results with only CO at the inlet

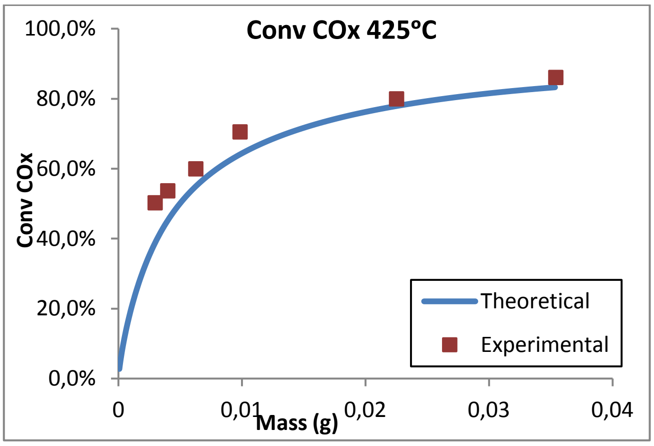

Figure 7: Comparison between the prevision of the conversion of COx at 425ºC by the kinetic model and the experimental results with an equimolar mixture of CO and CO_2 at the inlet

The simulation made considered an isothermal reactor, however, that is not entirely true as there is heat transfer through the walls and convection inside and outside of the catalytic bed.

In a new simulation it was taken into account the heat transferred through the walls considering the thermal conductivity of pirex glass. The convection was neglected as in all experiments the catalyst was diluted in SiC, a component that allows the uniformity of temperature maintaining isothermal conditions. It was showed a fast increase of the temperature in the first layers of the catalytic bed followed by its slower decrease as exemplified in Figs. 8 and 9. In the cases were the mass of catalyst present in the reactor was bigger, the temperature at the outlet assumed the same value as the inlet; if the reactor had a smaller mass, the outlet temperature was about 5ºC higher.

It can be concluded the first layers of the catalytic bed are the most important part to occur the reaction, while the end acts as a diluent of the temperature.

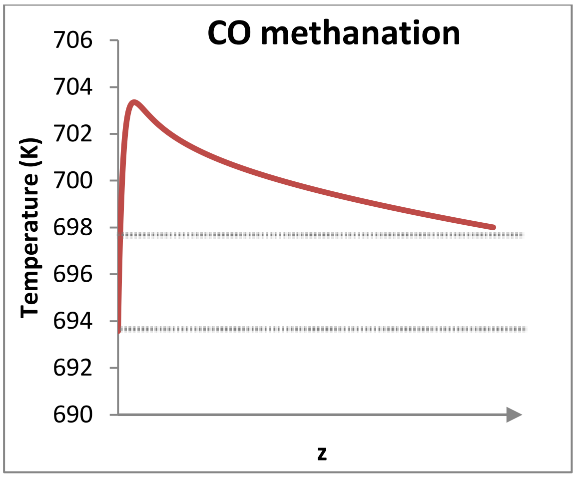

Figure 8: Profile temperature of CO methanation at a conversion of 45% at 425ºC with a low mass

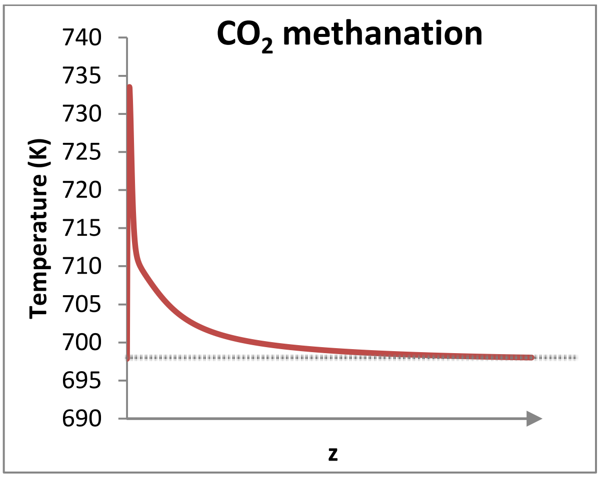

Figure 9: Profile temperature of CO_2 methanation at a conversion of 79% at 425ºC with a high mass

4 Conclusions

The characterization realized permitted to choose the best reduction treatment of the catalyst and to know its structural properties. After, the kinetic studies performed allowed to understand the influence of the reactants and products in the reactions and they were tested in the models found in the literature. It was concluded the model of Wheeler *et al* was the best to describe the kinetics of CO and CO_2 methanation. In terms of reverse water-gas shift reaction, as it is not affected by changes of hydrogen at the inlet, it was supposed to follow a redox model. This model showed a good fit of the experimental data and was in agreement with the supposition concerning the nature of adsorption of the other components. The kinetic constants present in the model were calculated and adjusted in a simulation of an isothermal plug flow reactor to better describe the results expected.

Then, it was simulated a polytropic plug flow reactor to evaluate the temperature behaviour inside the catalytic bed, and it was verified a strong increase of temperature in the first layers of the catalytic bed and then its fast decreasing to the inlet values. This suggests a high reactivity in the beginning of the catalytic bed while the end acts more like a thermal diluent.

Through the results obtained it can be concluded the catalyst is more reactive to CO when there is a mixture of CO_2 and CO at the inlet, being necessary less mass to reach the thermodynamic equilibrium.

References

[1] T. Schaaf, J. Grünig, M. R. Schuster, T. Rothenfluh e A. Orth, “Methanation of CO2 - storage of renewable energy in a gas distribution system,” *Energy, Sustainability and Society - SpringerOpen Journal,* pp. 1-14, 2014.

[2] C. H. Bartholomew e G. D. Weatherbee, “Hydrogenation of CO2 on Group VIII Metals - Kinetics and Mechanism of CO2 Hydrogenation on Nickel,” *Journal of Catalysis,* vol. 77, pp. 460-472, 1982.

[3] J. Xu e G. F. Froment, “Methane Steam Reforming, Methanation and Water-Gas Shift: I. Intrinsic Kinetics,” *AIChE Journal,* vol. 35, n.º 1, pp. 88-96, January 1989.

[4] C. Wheeler, A. Jhalani, E. J. Klein, S. Tummala e L. D. Schmidt, “The water-gas-shift reaction at short contact times,” *Journal of Catalysis,* vol. 223, pp. 191-199, 2004.